

## Cooperative Effects in Closely Packed Quantum Emitters with Collective Dephasing

B. Prasanna Venkatesh,<sup>1,2</sup> M. L. Juan,<sup>1,3</sup> and O. Romero-Isart<sup>1,2</sup>

<sup>1</sup>*Institute for Quantum Optics and Quantum Information of the Austrian Academy of Sciences, A-6020 Innsbruck, Austria*

<sup>2</sup>*Institute for Theoretical Physics, University of Innsbruck, A-6020 Innsbruck, Austria*

<sup>3</sup>*Institute for Experimental Physics, University of Innsbruck, A-6020 Innsbruck, Austria*



(Received 15 June 2017; published 19 January 2018)

In a closely packed ensemble of quantum emitters, cooperative effects are typically suppressed due to the dephasing induced by the dipole-dipole interactions. Here, we show that by adding sufficiently strong collective dephasing, cooperative effects can be restored. Specifically, we show that the dipole force on a closely packed ensemble of strongly driven two-level quantum emitters, which collectively dephase, is enhanced in comparison to the dipole force on an independent noninteracting ensemble. Our results are relevant to solid-state systems with embedded quantum emitters such as color centers in diamond and superconducting qubits in microwave cavities and waveguides.

DOI: [10.1103/PhysRevLett.120.033602](https://doi.org/10.1103/PhysRevLett.120.033602)

A collection of two-level quantum emitters (TLEs) with subwavelength average separations can show remarkable cooperative behavior like superradiant emission [1–3]. The study of optical response in such systems has predominantly been restricted to the emission properties or the propagation of light within the TLE ensemble. This is because the systems usually considered in the early days [2,4], as well as in some recent works [5–8], are gaseous clouds of atoms. With the advent of artificial atoms in solid-state systems, e.g., quantum dots [9], superconducting qubits [10,11], and color centers in diamond [12–14], it is now possible to study the impact of cooperative effects on other aspects of the optical response. For example, a recent experiment [13] studied the dipole force on optically trapped nanodiamonds containing a high density of nitrogen vacancy centers. An intriguing result in Ref. [13] was that the observed dipole force originating from the emitters could not be correctly accounted for by considering the emitters to respond independently.

In this Letter, we focus on cooperative effects in a small and closely packed ensemble of TLEs subject to strong coherent driving and collective dephasing. Specifically, we show that the dipole force on such an ensemble can be larger than on an equivalent one where each TLE spontaneously emits *independently*. For the emitter separations that we consider here, the dipole-dipole interaction can be larger than the linewidth of the individual emitters. Furthermore, spontaneous emission is not perfectly collective. In this situation, one typically expects cooperative effects to be suppressed [2,15]. Here, we show that the combination of strong driving and large collective dephasing can restore cooperative effects, even in the presence of dipole interaction shifts and noncollective spontaneous emission. While there have been previous studies of cooperative effects with strong driving fields [16–22], the role of collective dephasing has received less attention

[10,13]. In the context of quantum information, collective decoherence in general—and collective dephasing in particular—has been studied both theoretically [23–25] and experimentally [26,27]. In those works, particular attention was paid to the existence and the robustness of so-called decoherence-free subspaces (DFS) under collective dephasing [25]. Moreover, recent studies [28,29] have shown that collective dephasing could also be used as a resource to generate strong but separable correlations. We note that, due to their promise as a general passive strategy to protect quantum resources from noise, the study of DFS continues to be an active area of research; see Ref. [30] for a recent review of the theoretical aspects and Ref. [31] for experimental implementations. Recently, novel applications of DFS, such as the generation of arbitrary photonic states [32] and universal quantum computation in waveguide QED [33], as well as quantum repeaters with trapped ions [34], have also been proposed.

Let us consider a collection of  $N$  identical TLEs with resonance frequency  $\omega_0 \equiv ck_0 \equiv 2\pi c/\lambda_0$ . The matrix element of the dipole moment operator  $\hat{\mathbf{d}}$  is given by  $\langle e|\hat{\mathbf{d}}|g\rangle \equiv \epsilon_a d$ , where  $|g\rangle$  ( $|e\rangle$ ) denotes the ground (excited) state and  $|\epsilon_a| = 1$ . For simplicity, we assume  $\epsilon_a$  and  $d$  to be real. The TLEs, each with position  $\mathbf{r}_m$  ( $m = 1, \dots, N$ ), are fixed on a background matrix with center-of-mass position  $\mathbf{x}$ , namely,  $\mathbf{r}'_m \equiv \mathbf{r}_m - \mathbf{x}$  for all values of  $m$  is a constant of motion. We consider the TLEs to be driven by a classical electromagnetic field of the form  $\mathbf{E}(\mathbf{r}, t) = \mathbf{E}(\mathbf{r}) \cos(\omega_d t) \equiv \epsilon_d E_0 f(\mathbf{r}) \cos(\omega_d t)$ , where  $\epsilon_d$  and  $E_0$  are real and  $|\epsilon_d| = 1$ . We assume that  $f(\mathbf{r}_m) \approx f(\mathbf{x})$  for all values of  $m$ . In a frame rotating with the drive and assuming the rotating wave approximation, the Hamiltonian describing the interaction of the identical TLEs with  $\mathbf{E}(\mathbf{r}, t)$  is given by

$$\hat{H}_A \equiv \frac{\hbar\Omega(\mathbf{x})}{2} \hat{S}^x - \frac{\hbar\Delta}{2} \hat{S}^z. \quad (1)$$

Here,  $\Omega(\mathbf{x}) \equiv -2dE_0(\mathbf{e}_a \cdot \mathbf{e}_d)f(\mathbf{x})/\hbar$  is the Rabi frequency and  $\Delta \equiv \omega_d - \omega_0$  the detuning. Hereafter, we use the following notation for the spin operators:  $\hat{\sigma}_m^\alpha$  denotes the Pauli matrix (for  $\alpha = x, y, z$ ) and the ladder operator (for  $\alpha = \pm$ ) of the  $m$ th TLE, and the collective operators are denoted by  $\hat{S}^\alpha \equiv \sum_{m=1}^N \hat{\sigma}_m^\alpha$ . Apart from the dynamics induced by the interaction with the external driving, we assume the TLEs to experience collective dephasing as well as dipole-dipole interaction and spontaneous emission due to the interaction with free electromagnetic field modes in the vacuum state. The overall dynamics of such an ensemble of identical TLEs can be then described by the master equation  $\dot{\hat{\rho}} = \mathcal{L}\hat{\rho} \equiv (\mathcal{L}_H + \mathcal{L}_\Gamma + \mathcal{L}_\gamma)\hat{\rho}$ , where [1–3]

$$\mathcal{L}_H\hat{\rho} \equiv \frac{1}{i\hbar}[\hat{H}_A + \hat{H}_I, \hat{\rho}], \quad (2)$$

$$\mathcal{L}_\Gamma\hat{\rho} \equiv \sum_{mn} \Gamma_{mn} (2\hat{\sigma}_m^- \hat{\rho} \hat{\sigma}_n^+ - \hat{\sigma}_m^+ \hat{\sigma}_n^- \hat{\rho} - \hat{\rho} \hat{\sigma}_m^+ \hat{\sigma}_n^-), \quad (3)$$

$$\mathcal{L}_\gamma\hat{\rho} \equiv -\frac{\gamma_c}{4} [\hat{S}^z, [\hat{S}^z, \hat{\rho}]]. \quad (4)$$

The term  $\mathcal{L}_H$  describes coherent dynamics given by the interaction with the external field, Eq. (1), and the dipole-dipole interaction given by  $\hat{H}_I \equiv \sum_{m \neq n} \hbar g_{mn} \hat{\sigma}_m^+ \hat{\sigma}_n^-$ , where [35]

$$g_{mn} \equiv -\frac{3\Gamma}{4} \left[ (1 - \cos^2\theta_{mn}) \frac{\cos\xi}{\xi} - (1 - 3\cos^2\theta_{mn}) \left( \frac{\cos\xi}{\xi^3} + \frac{\sin\xi}{\xi^2} \right) \right]. \quad (5)$$

Here,  $\xi = k_0 r_{mn} \equiv k_0 |\mathbf{r}_m - \mathbf{r}_n|$ , and  $\cos\theta_{mn} \equiv (\mathbf{r}_m - \mathbf{r}_n) \cdot \mathbf{e}_a / r_{mn}$ . The term  $\mathcal{L}_\Gamma$  describes the spontaneous emission of the TLEs with correlated emission rates given by

$$\Gamma_{mn} \equiv \frac{3\Gamma}{4} \left[ (1 - \cos^2\theta_{mn}) \frac{\sin(\xi)}{\xi} - (1 - 3\cos^2\theta_{mn}) \left( \frac{\sin\xi}{\xi^3} - \frac{\cos\xi}{\xi^2} \right) \right]. \quad (6)$$

The diagonal term  $\Gamma_{mm} \equiv \Gamma/2 = 2d^2\omega_0^3/(3\hbar c^3)$  is the individual spontaneous emission rate of the TLEs. The term  $\mathcal{L}_\gamma$  describes collective dephasing with a rate given by  $\gamma_c$ . It is convenient to introduce the rate  $\bar{g} \equiv \sum_{n \neq 1} |g_{1n}|$ , which parametrizes the strength of the dipole-dipole interaction, and  $\bar{\Gamma} \equiv \sum_{n \neq 1} \Gamma_{1n}/(N-1)$ , which parametrizes the cooperativity of the spontaneous emission. The physical origin of collective dephasing is left unspecified in the theoretical treatment here. Note that it can, for instance, arise via correlated magnetic field fluctuations for ions [28], or due to interactions with phononic baths in the case of color centers [23,36,37] (see the Supplemental Material [38] for additional details regarding such situations).

We are interested in the closely packed regime defined by  $k_0 r_{mn} \leq 1$  for any pair of TLEs. While in this regime the spontaneous emission is predominantly collective, namely,  $\bar{\Gamma} \lesssim \Gamma/2$ , the strong dipole-dipole interaction  $\bar{g} \gg \Gamma$

typically suppresses any cooperative effect. However, we show below that strong collective dephasing  $\gamma_c \gg \Gamma$  together with strong driving  $\Omega(\mathbf{x}) \gg \Gamma$  can recover cooperative effects. We concentrate in particular on the steady state value of  $\hat{S}^x$ , namely,  $\langle \hat{S}^x \rangle \equiv \text{tr}[\hat{S}^x \hat{\rho}_s]$ , where  $\mathcal{L}\hat{\rho}_s = 0$ . This is related to the dipole force exerted by the driving field to the matrix hosting the TLEs. Indeed, assuming that the motion of the background matrix in the applied field is slow compared to the emitter dynamics, the dipole force is given by

$$\mathbf{F}_{\text{dp}} = -\frac{\hbar \nabla \Omega(\mathbf{x})|_{\mathbf{x}_0}}{2} \langle \hat{S}^x \rangle, \quad (7)$$

where  $\mathbf{x}_0$  is the equilibrium position of the matrix. For an ensemble of  $N$  independent TLEs, namely, with  $g_{mn} \equiv 0$  and  $\Gamma_{mn} \equiv 0$  (for  $m \neq n$ ), one has

$$\begin{aligned} \langle \hat{S}^x \rangle_{\text{ind}} &= N \frac{4\Delta\Omega_0\Gamma}{\Gamma(4\Delta^2 + \gamma_\perp^2) + 2\Omega_0^2\gamma_\perp} \\ &\leq N \frac{\Omega_0\Gamma}{\sqrt{\Gamma\gamma_\perp(\Gamma\gamma_\perp + 2\Omega_0^2)}}. \end{aligned} \quad (8)$$

Here,  $\Omega_0 \equiv \Omega(\mathbf{x}_0)$ ,  $\gamma_\perp \equiv (\Gamma + 2\gamma_c)$ , and the upper bound is achieved at the optimal detuning

$$\Delta_0 \equiv -\sqrt{\frac{\gamma_\perp(\Gamma\gamma_\perp + 2\Omega_0^2)}{4\Gamma}}. \quad (9)$$

We are interested in the parameter  $\eta \equiv \langle \hat{S}^x \rangle / \langle \hat{S}^x \rangle_{\text{ind}}$  evaluated at  $\Delta = \Delta_0$  (note that  $\langle \hat{S}^x \rangle$  is not maximized at  $\Delta_0$ ). Specifically, we refer to situations when  $\eta > 1$  as *cooperative enhancement* (CE). We remark that, since we are interested in closely packed ensembles, we do not consider variations of the Rabi frequency with emitter locations  $\mathbf{r}_m$ , which can also lead to interesting modifications of collective effects [44,45].

Let us consider  $N$  identical TLEs, randomly positioned in a three-dimensional volume with an average separation given by  $\bar{r} \equiv \sum_{m>n} r_{mn}/N$ ; see Fig. 1(a). We generate multiple random configurations at a fixed value of  $\bar{r}$  using the procedure described in Ref. [46] (see the Supplemental Material [38] for details) and numerically calculate  $\hat{\rho}_s$  in each case using Ref. [47]. The average  $\eta$  value over 1000 configurations is plotted in Fig. 1(b) as a function of  $\bar{r}/\lambda_0$  for  $N = 6$  with (solid line) and without (dotted line) collective dephasing. The shaded regions correspond to the interval where a majority, 68%, of the values for  $\eta$  lie. In the absence of collective dephasing ( $\gamma_c = 0$ ), there is no CE ( $\eta \leq 1$ ). However, in the presence of strong collective dephasing ( $\gamma_c/\Gamma \approx 10^4$ ) and strong driving ( $\Omega_0/\Gamma = 10^3$ ), there is a range of separations  $\bar{r}$  where there is CE ( $\eta > 1$ ). This is the main finding of this Letter. In the inset of Fig. 1(b), the parameters  $\bar{g}/\Gamma$  and  $2\bar{\Gamma}/\Gamma$  as a function of  $\bar{r}$  (averaged over 1000 configurations) are plotted. Note that CE vanishes both at large average separations due to the noncollective nature

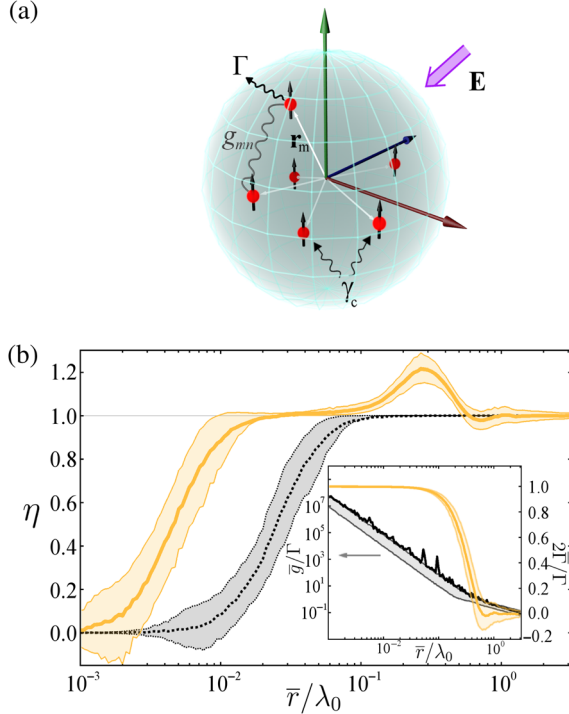


FIG. 1. (a) Schematic illustration of a driven ensemble of randomly distributed identical TLEs in a 3D volume. (b)  $\eta$  is plotted as a function of  $\bar{r}/\lambda_0$  for  $N = 6$ . The thick lines are the mean  $\eta$  over 1000 random distributions and the shaded areas represent regions where 68% of the values for  $\eta$  lie (see [38] for further details). Solid (dotted) line corresponds to  $\gamma_c/\Gamma = 1.3 \times 10^4$  ( $\gamma_c = 0$ ) for  $\Omega_0/\Gamma = 10^3$ . Inset plots the mean and the 68% confidence interval of  $\bar{g}/\Gamma$  and  $2\bar{\Gamma}/\Gamma$  as a function of  $\bar{r}/\lambda_0$ .

of spontaneous emission and at small distances due to the large dipole-dipole interaction.

Let us analytically support these statements for the simplest  $N = 2$  case [15]. The Hamiltonian including the dipole interaction is

$$\mathcal{L}_H \hat{\rho} \equiv \frac{1}{21} [\Omega_0 \hat{S}^x - (\Delta_0 + \bar{g}) \hat{S}^z + 2\bar{g} \hat{S}^+ \hat{S}^-, \hat{\rho}]. \quad (10)$$

In this case, the Hamiltonian is collective and commutes with  $\hat{S}^2$ . By contrast, in the finite emitter separation regime, where the so-called small sample limit [1,2,16,22,48] cannot be used, the spontaneous emission equation (3) is still noncollective, i.e.,  $\chi \equiv 2\bar{\Gamma}/\Gamma < 1$ . Following Ref. [15] and as shown in the Supplemental Material [38], one can analytically calculate  $\eta$ . Figure 2 plots the CE region ( $\eta > 1$ ) in the plane  $(\Omega_0/\Gamma, \gamma_c/\Gamma)$  for different values of  $\bar{r}$ . Note that CE requires both large dephasing and large driving. Furthermore, from the lengthy analytical expression for  $\eta$ , one can obtain that, in the limit of large dephasing,  $\eta$  reads

$$\lim_{\gamma_c/\Gamma \rightarrow \infty} (\eta - 1) \sim \frac{\Gamma}{\gamma_c} \frac{\chi}{2(1+\chi)} \left( \frac{\Omega_0^2}{\Gamma^2} - 1 - \chi \right). \quad (11)$$

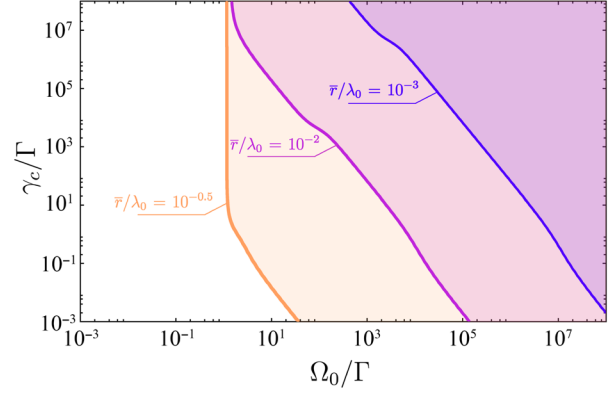


FIG. 2. Regions of CE for  $N = 2$  in the plane  $(\Omega_0/\Gamma, \gamma_c/\Gamma)$  for different values of  $\bar{r}/\lambda_0$ . The contour line corresponds to  $\eta = 1$ .

In this limit, CE ( $\eta > 1$ ) requires sufficiently large driving:  $\Omega_0 > \sqrt{\Gamma^2 + 2\bar{\Gamma}}$ . Alternatively, one can also show that, in the limit of no dephasing ( $\gamma_c = 0$ ) and large driving,  $\eta$  reads

$$\lim_{\Omega_0/\Gamma \rightarrow \infty, \gamma_c=0} (\eta - 1) \sim -\frac{\Gamma^2}{\Omega_0^2} \frac{1}{8} \left( \chi^2 + 2\chi + \frac{4\bar{g}^2}{\Gamma^2} \right), \quad (12)$$

and hence there is no CE ( $\eta < 1$ ). This is in agreement with previous studies of resonance fluorescence [16–18,22] at strong driving, which results from the increased occupation of the bright Dicke subspace in the small sample limit. It was shown in Ref. [15] that when  $\chi < 1$ , such an enhancement is absent. Interestingly, we claim here that large collective dephasing can restore cooperative effects.

Returning to Fig. 1(b),  $N = 6$ , we observe that there is an optimal separation distance  $\bar{r}/\lambda_0$  where  $\eta$  reaches a maximum. In general, the dipole-dipole interactions for  $N > 2$  do not conserve permutation symmetry. As a result, large dipole interactions induce strong local dephasing, apart from providing energy shifts, that prevent the TLEs to be polarized at the chosen detuning  $\Delta_0$ . We see in Fig. 1(b) that, in regions with CE, the dipole interactions satisfy  $\gamma_c \gg \bar{g} \sim \Gamma$ . In this manner we can understand the maximum  $\eta$  in Fig. 1(b) as occurring at separations where the dipole interactions are small enough to not dephase the collective behavior fostered by the cooperative spontaneous emission and collective dephasing. This statement can be quantified by noting that the product  $g_{12}(1 - 2\Gamma_{12}/\Gamma)$ , for a pair of TLEs with parallel moments and  $\theta_{12} = \pi/2$ , is locally minimized at  $r_{12} \approx 0.2\lambda_0$ . This is consistent with the position of the peak in Fig. 1(b). Furthermore, this also agrees with the observation that the location of the peak remains in the same density region for various ensemble sizes (see Fig. 3) and driving strengths  $\Omega_0$  (see the Supplemental Material [38]).

For  $N > 6$ , an exact numerical calculation of  $\hat{\rho}_s$  becomes rapidly intractable with standard resources. State-of-the-art approximation methods in the field, such as Holstein-Primakoff [49–51] or extended mean field [52], are not valid in the strong driving ( $\Omega_0 \gg \Gamma$ ) and

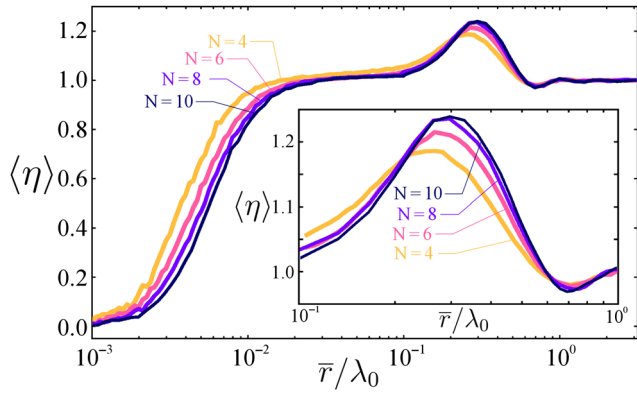


FIG. 3.  $\langle \eta \rangle$  is plotted as a function of  $\bar{r}/\lambda_0$  for different values of  $N$  using a rate equation approximation for  $\bar{r}/\lambda_0 < 10^{-1}$  (averaged over 400 random configurations) and using a trajectory method simulation (averaged over 200 configurations)  $\bar{r}/\lambda_0 > 10^{-1}$ . (Inset) Enlargement of the region of CE.

strong dipole-dipole interaction ( $\bar{g} \gg \Gamma$ ) regimes, respectively. The separation of time scales between the spontaneous emission and collective dephasing  $\gamma_c \gg \Gamma$  also makes trajectory methods [53] unsuitable. For small emitter separations up to  $\bar{r}/\lambda_0 \sim 10^{-1}$ , we find that a numerical diagonalization of the Hamiltonian  $\hat{H}_A + \hat{H}_I$  followed by a secular approximation to convert the master equation to a rate equation in the dressed basis [54] allows us to go up to  $N = 10$  emitters. For  $\bar{r}/\lambda_0 \gtrsim 10^{-1}$  the weak dipole-dipole interactions do not appreciably lift the degeneracy between the Dicke states with the same angular momentum projection  $m$  but different total angular momentum  $S$ , rendering the dressed approach invalid. In this regime we proceed as follows. The Liouvillian of the master equation can be written as  $\mathcal{L} = \mathcal{L}_0 + \mathcal{L}_1$ , where  $\mathcal{L}_0 \hat{\rho} \equiv \mathcal{L}_\gamma \hat{\rho} + i\Delta_0[\hat{S}^z, \hat{\rho}]/2$  and  $\mathcal{L}_1 \equiv \mathcal{L}_\Gamma \hat{\rho} + (i\hbar)^{-1}[\hat{H}_I + \hbar\Omega_0 \hat{S}^x/2, \hat{\rho}]$ . In most of the regime where  $\eta > 1$ , one has it that  $\gamma_c$  and  $\Delta_0$  are much larger than  $\bar{\Gamma}$ ,  $\bar{g}$ , and  $\Omega_0$ . Indeed, note that  $\Delta_0 \approx \Omega_0 \sqrt{\gamma_c/\Gamma}$  when  $\Omega_0^2 \gg \Gamma\gamma_c$ , which, according to Eq. (11), is required to have an appreciable value of  $\eta - 1 > 0$ . Under these assumptions,  $\mathcal{L}_0$  describes faster dynamics than  $\mathcal{L}_1$ , and hence one can adiabatically eliminate [55,56] the fast dynamics. This leads to an effective master equation in the dark subspace of  $\mathcal{L}_0$ , namely, for states  $\hat{\mu}$  such that  $\mathcal{L}_0 \hat{\mu} = 0$ . As shown in the Supplemental Material [38], the effective master equation is given by

$$\dot{\hat{\mu}} = \frac{1}{i\hbar}[\hat{H}_I, \hat{\mu}] + \mathcal{L}_\Gamma \hat{\mu} - \frac{\kappa}{4}([\hat{S}^-, [\hat{S}^+, \hat{\mu}]] + [\hat{S}^+, [\hat{S}^-, \hat{\mu}]]) \quad (13)$$

Here,  $\kappa \equiv \Omega_0^2 \gamma_c / (\gamma_c^2 + \Delta_0^2)$  is on the order of  $\Gamma$  in the assumed parameter regime. Equation (13) can be conveniently solved numerically via trajectory unravelling [53].

In Fig. 3, the results for the averaged  $\eta$  over multiple random configurations,  $\langle \eta \rangle$ , for eight and ten TLEs are presented. For  $\bar{r}/\lambda_0 < 10^{-1}$ ,  $\langle \eta \rangle$  was calculated by averaging over 400 random configurations, with steady states calculated using the rate equation method. For  $\bar{r}/\lambda_0 > 10^{-1}$ , the mean was calculated over 200 configurations from the steady state solutions determined by averaging over 500 trajectories each [47].

The statistical distribution of  $\eta$  and checks to ensure that the approximate methods used for  $N = 8, 10$  in Fig. 3 agree with the exact results for  $N \leq 6$  are presented in the Supplemental Material [38]. From the inset in Fig. 3, we see that while  $\langle \eta \rangle$  increases with  $N$  in the CE region up to  $N = 8$ , there is no appreciable gain for  $N = 10$ . In the Supplemental Material [38], we also demonstrate CE for an equidistant circular arrangement of TLEs. Since dipole-dipole interactions are permutation symmetric in this case, we find a significant CE also at smaller separations than in the random arrangement. We remark that the choice of detuning  $\Delta_0$  maximizes  $\langle S^x \rangle$  for independent emitters and that, hence, an optimized choice for the collective case can certainly lead to even larger  $\eta$ . A more systematic study of the CE as a function of different arrangements of TLEs [35], as well as the development of efficient methods to numerically and analytically address larger number of TLEs, is left for future work.

We conclude with some remarks relating our findings to the recent studies of dipole force on color centers embedded in nanodiamonds [13,14]. In the experiment [13], the underlying mechanism for the large dephasing at room temperature is mediated via phonon interactions [36] and consequently changes rapidly with the temperature of the lattice. Since we have demonstrated that the presence of large collective dephasing is crucial to the observation of the enhanced dipole force, this raises the prospect of repeating the experiment [13], or even lifetime measurements in Ref. [14], at lower temperatures. At lower temperatures, the dephasing will be reduced, which should lead to a strong modification—or even suppression—of collective effects. This is counterintuitive to the study of collective effects in atomic systems. In connection with the proposal for levitated optomechanics with nanodiamonds [57] (as well as other proposals [58] concerning collective effects in optomechanics), it would be interesting to explore whether collective effects in dense ensembles would lead to polarizabilities comparable to or greater than the bulk polarizability of the embedding medium. A promising direction for further research would be to explore other scenarios where large collective dephasing restores cooperative effects. Remarkably, in systems such as superconducting qubits [10,11] where the collective dephasing can be externally controlled, this could allow us to observe cooperative effects even in the presence of inhomogeneities and dipole shifts.



This work is supported by the Austrian Federal Ministry of Science, Research and Economy (BMWFV). We acknowledge our discussions with J. I. Cirac, J. J. Garcia-Ripoll, C. Gonzalez-Ballester, G. Kirchmair, H. Ritsch, and B. Vermersch.

- 
- [1] G. S. Agarwal, in *Quantum Optics*, edited by G. Höhler, Springer Tracts in Modern Physics Vol. 70 (Springer, Berlin, 1974), Doi: 10.1007/BFb0042382.
- [2] M. Gross and S. Haroche, *Phys. Rep.* **93**, 301 (1982).
- [3] Z. Ficek, R. Tanas, and S. Kielich, *Physica (Amsterdam)* **146A**, 452 (1987).
- [4] M. S. Malcuit, J. J. Maki, D. J. Simkin, and R. W. Boyd, *Phys. Rev. Lett.* **59**, 1189 (1987).
- [5] R. Bachelard, N. Piovela, and Ph. W. Courteille, *Phys. Rev. A* **84**, 013821 (2011).
- [6] W. Guerin, M. O. Araújo, and R. Kaiser, *Phys. Rev. Lett.* **116**, 083601 (2016).
- [7] M. O. Araújo, I. Krešić, R. Kaiser, and W. Guerin, *Phys. Rev. Lett.* **117**, 073002 (2016); S. J. Roof, K. J. Kemp, M. D. Havey, and I. M. Sokolov *ibid.* **117**, 073003 (2016).
- [8] S. Jennewein, M. Besbes, N. J. Schilder, S. D. Jenkins, C. Sauvan, J. Ruostekoski, J.-J. Greffet, Y. R. P. Sortais, and A. Browaeys, *Phys. Rev. Lett.* **116**, 233601 (2016); S. D. Jenkins, J. Ruostekoski, J. Javanainen, S. Jennewein, R. Bourgain, J. Pellegrino, Y. R. P. Sortais, and A. Browaeys, *Phys. Rev. A* **94**, 023842 (2016).
- [9] T. Brandes, *Phys. Rep.* **408**, 315 (2005).
- [10] F. Nissen, J. M. Fink, J. A. Mlynek, A. Wallraff, and J. Keeling, *Phys. Rev. Lett.* **110**, 203602 (2013).
- [11] J. A. Mlynek, A. A. Abdumalikov, Jr., C. Eichler, and A. Wallraff, *Nat. Commun.* **5**, 5186 (2014).
- [12] M. W. Doherty, N. B. Manson, P. Delaney, F. Jelezko, J. Wrachtrup, and L. C. L. Hollenberg, *Phys. Rep.* **528**, 1 (2013); Y. Chu and M. D. Lukin, in *Quantum Optics and Nanophotonics*, Lecture Notes of the Les Houches Summer School 2013 Session C1, edited by Claude Fabre, Vahid Sandoghdar, Nicolas Treps, and Leticia F. Cugliandolo (Oxford University Press, New York, 2017).
- [13] M. L. Juan, C. Bradac, B. Besga, G. Molina-Terriza, and T. Volz, *Nat. Phys.* **13**, 241 (2017).
- [14] C. Bradac, M. Johnsson, M. van Breugel, B. Baragiola, R. Martin, M. L. Juan, and G. Brennen, T. Volz, *Nat. Comm.* **8**, 1205 (2017).
- [15] Z. Ficek, R. Tanas, and S. Kielich, *Opt. Acta* **30**, 713 (1983).
- [16] A. S. Jahangir Amin and J. G. Cordes, *Phys. Rev. A* **18**, 1298 (1978).
- [17] G. S. Agarwal, L. M. Narducci, D. H. Feng, and R. Gilmore, *Phys. Rev. Lett.* **42**, 1260 (1979).
- [18] G. S. Agarwal, R. Saxena, L. M. Narducci, D. H. Feng, and R. Gilmore, *Phys. Rev. A* **21**, 257 (1980).
- [19] P. D. Drummond and S. S. Hassan, *Phys. Rev. A* **22**, 662 (1980).
- [20] H. J. Carmichael, *J. Phys. B* **13**, 3551 (1980).
- [21] G. Campagno and F. Persico, *Phys. Rev. A* **25**, 3138 (1982).
- [22] Z. Ficek and R. Tanas, *Phys. Rep.* **372**, 369 (2002).
- [23] G. M. Palma, K.-A. Suominen, and A. K. Ekert, *Proc. R. Soc. A* **452**, 567 (1996).
- [24] L.-M. Duan and G.-C. Guo, *Quantum Semiclass. Opt.* **10**, 611 (1998).
- [25] D. A. Lidar and K. Birgitta Whaley, *Irreversible Quantum Dynamics*, edited by F. Benatti and R. Floreanini, Springer Lecture Notes in Physics Vol. 622 (Springer, Berlin, 2003), p. 83.
- [26] P. G. Kwiat, A. J. Berglund, J. B. Altepeter, and A. G. White, *Science* **290**, 498 (2000).
- [27] D. Kielpinski, V. Meyer, M. A. Rowe, C. A. Sackett, W. M. Itano, C. Monroe, and D. J. Wineland, *Science* **291**, 1013 (2001).
- [28] B. P. Lanyon, P. Jurcevic, C. Hempel, M. Gessner, V. Vedral, R. Blatt, and C. F. Roos, *Phys. Rev. Lett.* **111**, 100504 (2013).
- [29] E. G. Carnio, A. Buchleitner, and M. Gessner, *Phys. Rev. Lett.* **115**, 010404 (2015).
- [30] D. Lidar, *Adv. Chem. Phys.* **154**, 295 (2014).
- [31] C. F. Roos, M. Chwalla, K. Kim, M. Riebe, and R. Blatt, *Nature (London)* **443**, 316 (2006); D. A. Pushin, M. G. Huber, M. Arif, and D. G. Cory, *Phys. Rev. Lett.* **107**, 150401 (2011); M. Friesen, J. Ghosh, M. A. Eriksson, and S. N. Coppersmith, *Nat. Commun.* **8**, 15923 (2017); F. Wang, Y.-Y. Huang, Z.-Y. Zhang, C. Zu, P.-Y. Hou, X.-X. Yuan, W.-B. Wang, W.-G. Zhang, L. He, X.-Y. Chang, and L.-M. Duan, *Phys. Rev. B* **96**, 134314 (2017); M. A. Perlin, Z.-Y. Wang, J. Casanova, and M. B. Plenio, *arXiv*: 1708.09414.
- [32] A. González-Tudela, V. Paulisch, D. E. Chang, H. J. Kimble, and J. I. Cirac, *Phys. Rev. Lett.* **115**, 163603 (2015).
- [33] V. Paulisch, H. J. Kimble, and A. González-Tudela, *New J. Phys.* **18**, 043041 (2016).
- [34] M. Zwerger, B. P. Lanyon, T. E. Northup, C. A. Muschik, W. Dür, and N. Sangouard, *Quant. Sci. Technol.* **2**, 044001 (2017).
- [35] S. Krämer, L. Ostermann, and H. Ritsch, *Europhys. Lett.* **114**, 14003 (2016).
- [36] K.-M. C. Fu, C. Santori, P. E. Barclay, L. J. Rogers, N. B. Manson, and R. G. Beausoleil, *Phys. Rev. Lett.* **103**, 256404 (2009).
- [37] A. Albrecht, A. Retzker, F. Jelezko, and M. B. Plenio, *New J. Phys.* **15**, 083014 (2013).
- [38] See Supplemental Material at <http://link.aps.org/supplemental/10.1103/PhysRevLett.120.033602>, which includes Refs. [39–43], for additional details on how the random configurations are generated, the analytical calculation of  $\eta$  for  $N = 2$  TLEs, derivation of the effective master equation, and some additional numerical results not presented in the Letter.
- [39] D. A. Lidar, Z. Bihary, and K. Birgitta Whaley, *Chem. Phys.* **268**, 35 (2001).
- [40] H.-P. Breuer and F. Petruccione, *The Theory of Open Quantum Systems* (Oxford University Press, Oxford, 2002).
- [41] H. J. Carmichael, *Statistical Methods in Quantum Optics I* (Springer, Berlin, 1999).
- [42] C. H. Kittel, *Introduction to Solid State Physics* (John Wiley & Sons, Singapore, 2004).
- [43] U. Dorner, *New J. Phys.* **14**, 043011 (2012).
- [44] H. Zoubi and H. Ritsch, *Europhys. Lett.* **90**, 23001 (2010).
- [45] A. Asenjo-Garcia, M. Moreno-Cardoner, A. Albrecht, H. J. Kimble, and D. E. Chang, *Phys. Rev. X* **7**, 031024 (2017).

- [46] F. Damanet and J. Martin, *J. Phys. B* **49**, 225501 (2016).
- [47] J. R. Johansson, P. D. Nation, and F. Nori, *Comput. Phys. Commun.* **184**, 1234 (2013).
- [48] R. H. Dicke, *Phys. Rev.* **93**, 99 (1954).
- [49] S. D. Jenkins and J. Ruostekoski, *Phys. Rev. A* **86**, 031602 (2012).
- [50] R. J. Bettles, S. A. Gardiner, and C. S. Adams, *Phys. Rev. Lett.* **116**, 103602 (2016).
- [51] M. D. Lee, S. D. Jenkins, and J. Ruostekoski, *Phys. Rev. A* **93**, 063803 (2016).
- [52] S. Krämer and H. Ritsch, *Eur. Phys. J. D* **69**, 282 (2015).
- [53] J. P. Clemens, L. Horvath, B. C. Sanders, and H. J. Carmichael, *Phys. Rev. A* **68**, 023809 (2003).
- [54] J. Dalibard and C. Cohen-Tannoudji, *J. Opt. Soc. Am. B* **2**, 1707 (1985).
- [55] J. I. Cirac, R. Blatt, P. Zoller, and W. D. Phillips, *Phys. Rev. A* **46**, 2668 (1992).
- [56] I. Lesanovsky and J. P. Garrahan, *Phys. Rev. Lett.* **111**, 215305 (2013).
- [57] M. L. Juan, G. Molina-Terriza, T. Volz, and O. Romero-Isart, *Phys. Rev. A* **94**, 023841 (2016).
- [58] A. Xuereb, C. Genes, and A. Dantan, *Phys. Rev. Lett.* **109**, 223601 (2012).